Photoluminescence spectra of polycrystalline ZnSe in different experimental geometries

[1] Abbasov I., [1] Musayev M., [2] Huseynov J., [3]Kostyrko M., [4] Babayev S., [4] Eyyubov G. and [5] Aliyeva S.

[1] Azerbaijan State Oil and Industry University, 20 Azadlig Street, 1010 Baku, Azerbaijan
[2] Azerbaijan State Pedagogical University, 68 Uzeyir Hajibeyli Street, 1000 Baku, Azerbaijan
[3] O. G. Vlokh Institute of Physical Optics, 23 Dragomanov Street, 79005 Lviv, Ukraine
[4] Institute of Physics of the NAS of Azerbaijan, 33 Huseyn Javid Avenue, 1141 Baku, Azerbaijan
[5] Baku State University, Nanotechnology Center, 23 Zahid Khalilov Street, 1148 Baku, Azerbaijan

Received: 10.03.2020

Abstract. We study the photoluminescence in polycrystalline ZnSe synthesized using a chemical vapour-deposition technique, which arises from excitation by the sources of different types and wavelengths. Two experimental geometries are used, which are related to the normal incidence of exciting radiation upon either polished or unpolished ZnSe surfaces. The excitation from the polished surface is carried out by the lasers with the wavelengths $\lambda_{ex} = 335$ and 325 nm (i.e., the photon energies higher than the bandgap, $h\nu_{ex} > E_g$), semiconductor lasers with $\lambda_{ex} = 532$, 642 and 785 nm (i.e., $h\nu_{ex} < E_g$) and a xenon lamp. The sample is also excited from the unpolished surface, using the lasers with $\lambda_{ex} = 325$ nm ($h\nu_{ex} > E_g$) and $\lambda_{ex} = 532$ nm ($h\nu_{ex} < E_g$), as well as the semiconductor laser with $\lambda_{ex} = 532$ nm ($h\nu_{ex} < E_g$). Following from our experimental results, we analyze and compare the edge (exciton) luminescence and the impurity-defect luminescence. Different behaviours of the luminescence spectra are observed, which depend on the type of excitation.

Keywords: polycrystalline zinc selenide, chemical vapour deposition-grown ZnSe, edge (exciton) and impurity-defect luminescence, photoluminescence spectra

UDC: 535.37

1. Introduction

Zinc selenide still remains the most promising wide-gap A_2B_6 material for semiconductor optoelectronics, including short-wavelength semiconductor electronic devices, display systems, LED technologies, X-ray detectors and lasers for transparency windows in the infrared region. Zinc selenide has a necessary set of physicochemical parameters which enable creating on its basis blue LEDs and the other blue light sources based on both spontaneous [1, 2] and stimulated [3] radiation. Studies of the luminescence in ZnSe provide information about the luminescence mechanisms and the parameters of recombination centres. Moreover, they enable also identifying technological conditions necessary for the synthesis of sufficiently high-quality crystalline samples with low concentrations of uncontrolled impurities.

The luminescent properties of the surface structures of crystalline substances have been extensively studied in the recent years [4–6]. They include most of the structures based on A_2B_6 compounds (e.g., thin films or grains of powder phosphors). Such structures are small in size (of the order of microns), whereas their electrical, photoelectric and optical properties are strongly influenced by electronic and molecular processes occurring on a surface. Specific properties of the

surface and, in particular, the existence of capture levels and surface barriers can affect strongly the luminescence of the structures under consideration. Any attempts to analyze and grasp the mechanisms of these processes need to solve a number of problems in both the physics and technology of luminescent materials, including those arising for the polycrystalline ZnSe grown with a common chemical vapour-deposition (CVD) method. Therefore, it would be interesting to compare the luminescence spectra detected for the same sample, which is excited from both polished and unpolished surfaces with different sources. The purpose of the present work is to perform complex experimental studies of the luminescence in CVD ZnSe arising from the excitation by the sources of different types and wavelengths in the two geometries. The latter are associated with normal incidence of the exciting quanta on either polished or unpolished surfaces of the same sample.

2. Methods and experiments

Polycrystalline CVD ZnSe sample with the thickness 3 mm was obtained by the CVD technique [7, 8]. It is known that crystal growth from the vapour phase occurs at a lower temperature, if compared with that typical for the melt technology. This reduces concentration of bulk defects and contamination of a growing crystal with the material of ampoule.

The luminescence spectra were studied in both the sub-surface layer and the bulk part of our sample. Different types of sources having different wavelengths were used to excite the luminescence. These were different harmonics of a solid-state laser (λ_{ex} = 335 and 532 nm), a helium–cadmium laser (λ_{ex} = 325 nm), semiconductor lasers (λ_{ex} = 532, 642 and 785 nm) and a xenon arc lamp. All the measurements were carried out at the room temperature. In fact, the use of different excitation sources with $h\nu_{ex} > E_g$ and $h\nu_{ex} < E_g$ allowed us to excite either sub-surface or bulk parts of the sample.

The photoluminescence (PL) spectra (see Fig. 1) were measured using an M833 double dispersive automated monochromator (the spectral resolution ~ 0.024 nm at the wavelength 600 nm). It had been controlled by a computer and equipped with a detector that recorded radiation

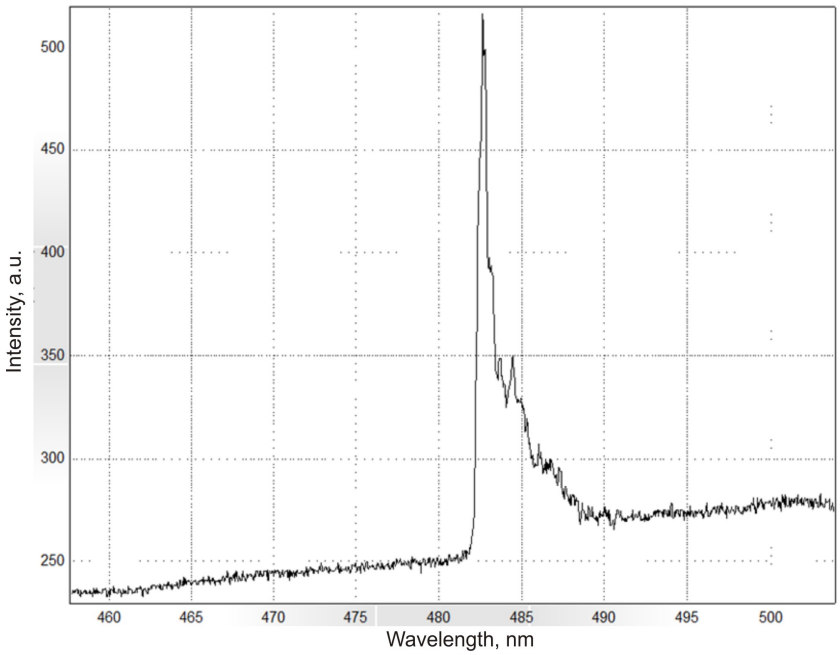

Fig. 1. Luminescence spectrum of polycrystalline CVD ZnSe (polished surface; λ_{ex} = 335 nm).

in the wavelength range 350÷2000 nm. An excitation radiation source was a pulsed Nd:YAG laser with built-in second and third harmonic generators designed to generate radiation with the wavelengths 1064, 532 and 335 nm. The laser pulse duration was 12 ns, with a maximum peak intensity ~ 10 MW/cm^2. In this case, the measurements were performed from the third harmonic, i.e. the wavelength λ_{ex} = 335 nm.

Luminescent properties of polycrystalline CVD ZnSe were also studied using a Varian Cary Eclipse spectrofluorimeter. A xenon lamp with an extended lifetime in a pulsed mode (the pulse width 2 μs and the power 75 kW) was used as a radiation source. The spectrofluorimeter monochromators had diffraction gratings with the parameters 1200 lines/mm and the software that enabled determining the wavelength with the accuracy up to 0.01 nm. The both monochromators had high-speed scanning capabilities. The instrument software allowed us to select different measurement modes and control the working elements. The emission spectra (see Fig. 2 and Fig. 3) were taken at the spectral slit width 2.5 nm. They were recorded in the range from 400 to 900 nm with the spectral resolution ~ 0.024 nm. The sample was excited by the light at the wavelengths λ_{ex} = 325, 330 and 350 nm ($hv_{ex} > E_g$).

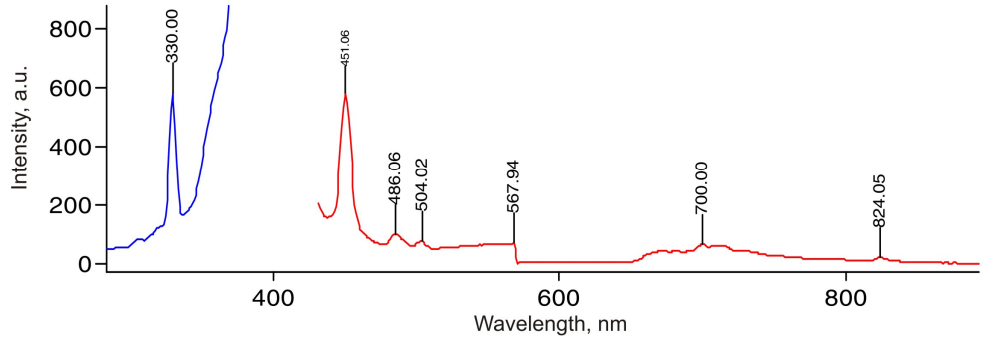

Fig. 2. Luminescence spectra of polycrystalline CVD ZnSe excited with a xenon lamp (polished surface; λ_{ex} = 330 nm).

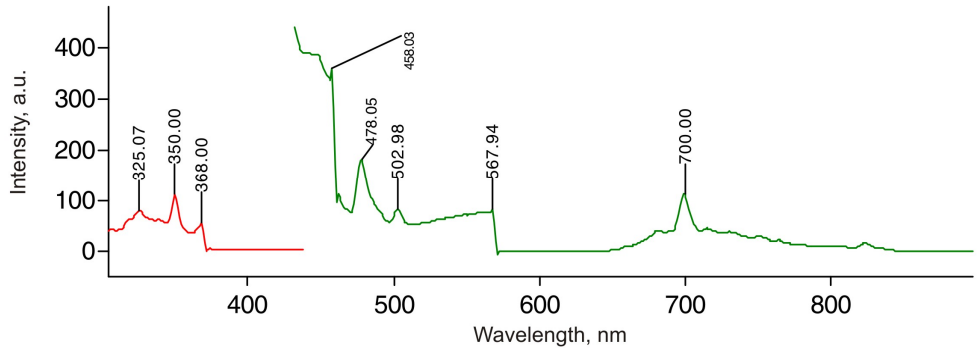

Fig. 3. Luminescence spectra of polycrystalline CVD ZnSe excited with a xenon lamp (polished surface; λ_{ex} = 325 nm and λ_{ex} = 350 nm).

Moreover, we studied the PL occurring after excitation by the continuous-wave He–Cd laser with the wavelength 325 nm (see Fig. 4 and Fig. 10) and the semiconductor lasers (λ_{ex} = 532 nm – see Fig. 5 and Fig. 9, λ_{ex} = 642 nm – see Fig. 6, and λ_{ex} = 785 nm – see Fig. 7). This luminescence was recorded using an MS5204i monochromator-spectrograph (SOL Instruments) with a diffraction grating 1800 lines/mm and ANDOR IDUS CCD detectors (DU420-OE and DU491A 1.7 models respectively for the visible and infrared ranges). The PL spectra were plotted after correcting them for the spectral sensitivity of our detecting system.

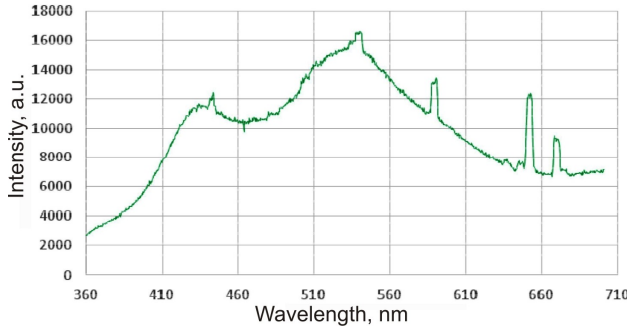

Fig. 4. Luminescence spectra of polycrystalline CVD ZnSe (polished surface; laser excitation at λ_{ex} = 325 nm).

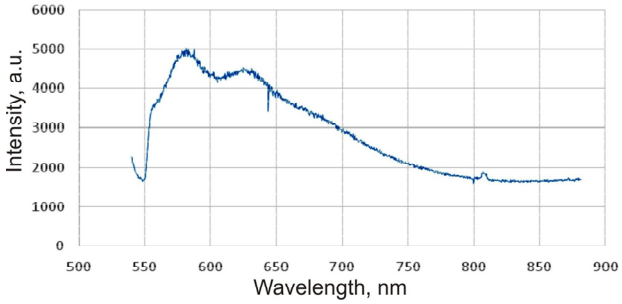

Fig. 5. Luminescence spectra of polycrystalline CVD ZnSe (polished surface; excitation with semiconductor laser at λ_{ex} = 532 nm).

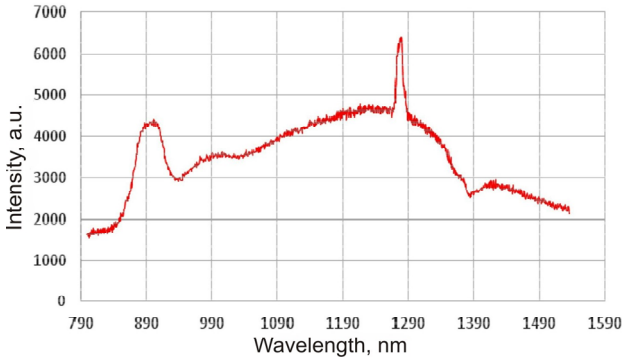

Fig. 6. Luminescence spectra of polycrystalline CVD ZnSe (polished surface; excitation with semiconductor laser at λ_{ex} = 642 nm).

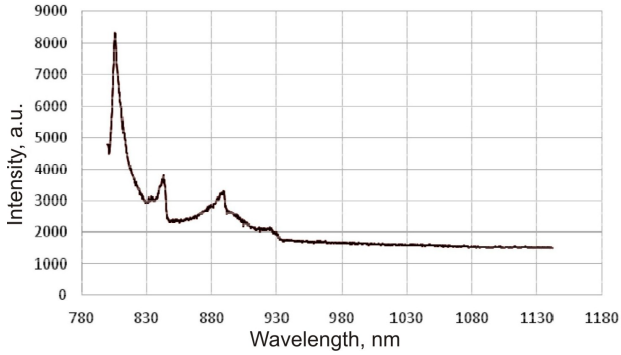

Fig. 7. Luminescence spectra of polycrystalline CVD ZnSe (polished surface; excitation with semiconductor laser at λ_{ex} = 785 nm).

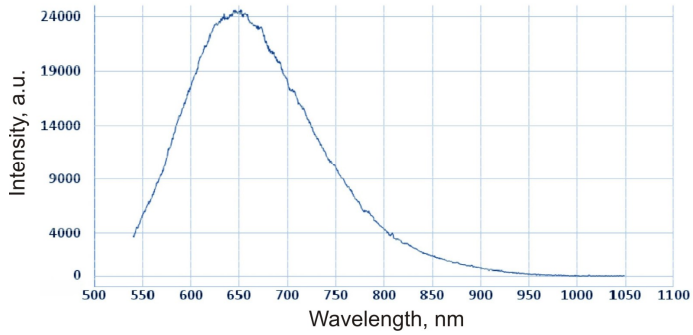

Fig. 8. Luminescence spectra of polycrystalline CVD ZnSe (unpolished surface; excitation with laser at λ_{ex} = 532 nm).

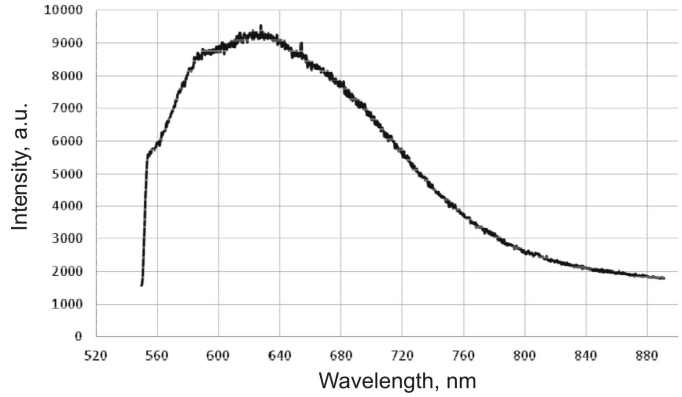

Fig. 9. Luminescence spectra of polycrystalline CVD ZnSe (unpolished surface; excitation with semiconductor laser at λ_{ex} = 532 nm).

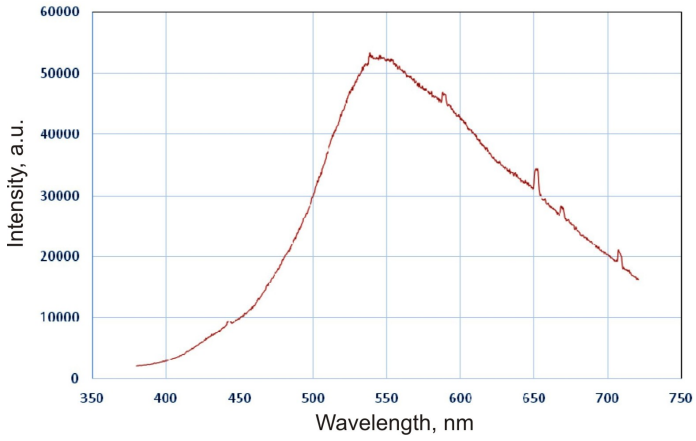

Fig. 10. Luminescence spectra of polycrystalline CVD ZnSe (unpolished surface; excitation with laser at λ_{ex}= 325 nm).

Finally, the luminescence studies from the unpolished surface (see Fig. 8) were carried out on a Nanofinder 30 Confocal micro-Raman spectrometer (Tokyo Instr., Japan). The second harmonic of the Nd:YAG laser with the radiation wavelength λ_{ex} = 532 nm and the maximal power 10 mW was used as an excitation source. The spectral resolution was not worse than ~ 0.014 nm. A cooled CCD camera with the resolution 1024×128 pixels operating in photon-counting mode served as a radiation detector. Finally, the luminescence spectra were recorded in the region λ = 440÷1500 nm.

3. Results and discussion

At first, the luminescence spectra have been measured from the polished surface of our sample (see the plots displayed from Fig. 1 to Fig. 7). The spectrum represented in Fig. 1 is obtained when the sample is excited by the third harmonic of the pulsed Nd:YAG laser (λ_{ex} = 335 nm, i.e. $h\nu_{ex} > E_g$). Several narrow lines with the maximum at 483 nm (2.57 eV) are observed in the spectrum. The difference of the bandgap and the maximum position is equal to 0.14 eV.

The luminescence spectra shown in Fig. 2 and Fig. 3 are recorded at the excitation with monochromatized radiation from the xenon lamp at the wavelengths λ_{ex} = 330, 325 and 350 nm ($h\nu_{ex} > E_g$). As Fig. 2 demonstrates, the luminescence intensity has maxima at several wavelengths: a narrow band located at λ_{max} = 451 nm and a number of narrow peaks at λ_{max} = 486, 504, 568, 700 and 824 nm. Fig. 2 presents the spectrum detected upon excitation with the wavelength 325 nm [Note that the same spectrum is obtained after excitation at 350 nm.] In these cases, narrow luminescence bands are observed at λ_{max} = 478 and 700 nm, and narrow peaks can be detected at λ_{max} = 503, 824, 568 and 458 nm. When compared with the spectra shown in Fig. 2, the only changes in the luminescence observed in Fig. 3 occur with the first and second maxima. The relative intensity and the energies of luminescence quanta decrease in the first maximum and increase in the second one. Furthermore, the spectra shown in Fig. 2 and Fig. 3 reveal the luminescence excitation spectra at the maxima corresponding to 451 and 700 nm. As seen from Fig. 2, the peak at 451 nm is the most efficiently excited by the light with the wavelength λ_{ex} = 330 nm, while the peak at 700 nm (see Fig. 3) with λ_{ex} = 325, 350 and 368 nm. For the luminescence which is not associated with the impurities or defects in the crystal structure, the luminescence excitation spectra involve no bands in the transparency range. In this spectral range, the luminescence is excited only in the region of long-wavelength fundamental absorption edge or upon the excitation by the light of which photon energy is higher than E_g.

In addition to the results presented above, we have also excited the luminescence with the radiation of the continuous-wave He–Cd laser (λ_{ex} = 325 nm, i.e. $h\nu_{ex} > E_g$ – see Fig. 4) and the continuous-wave semiconductor lasers with the wavelengths λ_{ex} = 532 nm (Fig. 5), λ_{ex} = 642 nm (Fig. 6) and λ_{ex} = 785 nm (Fig. 7). In the two latter cases we deal with the situation $h\nu_{ex} < E_g$. Under above excitation, we observe the luminescence peaks at λ_{max} = 431, 434 and 444 nm ('violet' peaks), a wide band at λ_{max} = 541 nm, peaks at λ_{max} = 591, 637, 645 and 668 nm (Fig. 4), wide bands at λ_{max} = 582 and 625 nm, peaks at λ_{max} = 631 and 808 nm (Fig. 5), wide bands at λ_{max} = 902, 970, 1230 and 1423 nm (Fig. 6), narrow bands at λ_{max} = 806, 833 and 843 nm, and a peak at λ_{max} = 889 nm (Fig. 7). Besides of these maxima, weak peaks are observed in Fig. 4 at 480, 505 and 512 nm.

All of the PL spectra presented above have been measured from the polished surface of our sample. On the contrary, Fig. 8, Fig. 9 and Fig. 10 show the spectra excited through a side face of the sample, i.e. its unpolished surface. The laser radiation with the wavelengths λ_{ex} = 532 and 325 nm (Fig. 8 and Fig. 10) and the semiconductor laser radiation with λ_{ex} = 532 nm (Fig. 9) have been used for excitation in these cases. After the excitation at λ_{ex} = 532 nm, a wide spectrum is detected with the half-width ~ 0.45 eV and a smeared maximum located at the wavelength 650 nm. Additionally, weak peaks are observed at 630, 670 and 810 nm. As a result of excitation with the continuous-wave semiconductor laser at λ_{ex} = 532 nm, we observe again a wide luminescence spectrum (see Fig. 9) with the half-width ~ 0.56 eV. It is 0.11 eV wider if compared with the spectrum obtained due to the other laser excitation (see Fig. 8). Under this condition, a self-activating luminescence band with the maximum located at 630 nm becomes dominant

(see Fig. 9). The spectrum also reveals very weak peaks situated at 650 and 810 nm. Moreover, a resonance excitation of the impurity state with the energy 2.22 eV (i.e., 560 nm) is observed in Fig. 9. Under the laser excitation λ_{ex} = 325 nm, we obtain the luminescence spectrum with the total half-width 0.69 eV. Here we deal with a wide band, with the maximum located at 540 nm and narrow peaks at 443, 590, 642, 645, 670, 710 and 730 nm (see Fig. 10). The main difference from the spectrum shown in Fig. 4, which has been obtained due to excitation from the polished surface of the sample by the same laser, consists in the absence of some peaks (430, 433, 480, 506 and 511 nm). Instead, new peaks appear at 710 and 730 nm.

According to the literature data, the edge luminescence associated with bound excitons dominates in the luminescence of undoped zinc selenide crystals in the region 440÷480 nm [4, 9–13]. Therefore, one can state that the narrow lines located at λ_{max} = 483 nm (2.57 eV – see Fig. 1) correspond to the luminescence of bound excitons. The edge luminescence is a result of radiative recombination of free electrons with holes, as well as free holes with electrons localized at the shallow donor centres in the singly positively charged selenium vacancies V_{Se}^{*}, of which depth is equal to about 0.02 eV [14]. In other words, they are formed due to the transitions with participation of interstitial selenium levels and its vacancies. Issuing from the 'extraction' method, the authors of Ref. [15] have suggested that the defects associated with hyper-stoichiometric selenium form the energy levels with the depth 0.13÷0.3 eV with respect to the ceiling of valence band.

The luminescence maxima corresponding to 451 nm (2.76 eV) and 486 nm (2.56 eV) in Fig. 2, as well as the peaks at 458 nm (2.71 eV) and 478 nm (2.6 eV) in Fig. 2 can also be considered as the luminescence linked with recombination of bound excitons. At the same time, the peak located at 444 nm (2.81 eV – see Fig. 4) is associated with stoichiometric Zn vacancies [4]. The peaks centred at 504 nm and 568 nm (Fig. 2 and Fig. 3), 541 nm and 591 nm (Fig. 4), and the band at 582 nm (Fig. 5) in the luminescence observed from both the polished and unpolished surfaces of our sample are, most likely, attributed to the existence of uncontrolled oxygen impurities (or Cu, Al). These maxima are associated with the complexes of intrinsic point defects (zinc interstitials Zn_i and zinc vacancies V_{Zn}) with oxygen or the other background impurities [12, 16, 17]. The luminescence maxima observed at 625 and 630 nm (see Fig. 5 and Fig. 8) and at 638, 645 and 670 nm (see Fig. 4 and Fig. 10) are due to recombination with participation of donor–acceptor pairs. Here doubly negatively charged vacancies $V_{zn}^{//}$ of zinc and singly positively charged vacancies V_{Se}^{*} of selenium can be responsible [9, 11, 18–20].

The presence of infrared bands in the luminescence of CVD ZnSe is testified by a peak located at 824 nm (Fig. 2 and Fig. 3), narrow bands at 806, 833 and 843 nm, a peak at 889 nm (Fig. 7), wide bands at 902, 970, 1230 and 1423 nm (Fig. 6), and a weak peak situated at 810 nm (Fig. 8). The authors of Refs. [9, 17, 21] have argued that these emission bands are associated with the vacancies V_{Se} of selenium. They have demonstrated that the intense bands located at 1230 and 1423 nm increase with increasing Se excess, i.e. with increasing concentration of zinc vacancies [V_{Zn}].

The PL spectra shown in Fig. 8 and Fig. 9 reveal wide PL bands, which represent sums of elementary bands with close wavelengths. These spectra are dominated by broad bands of self-activating luminescence with the maxima at 630 nm (Fig. 9) or at 650 nm (Fig. 8). According to the works [11, 18], a complex consisting of zinc vacancy and a shallow donor impurity can be responsible for this luminescence. However, the authors of Refs. [22–24] have recently suggested another model for the recombination luminescence centres, in which the two opposite recombination mechanisms associated with electrons and holes can simultaneously contribute to the effect. A possibility for localization of a free charge carrier in the vicinity of dipole centre

implies that either a free electron or a free hole can be localized in this centre whenever the crystal is excited (i.e., when the pairs of free electrons and holes are generated). Subsequent localization of carriers of the opposite signs at such recharged centres would lead to their recombination, which is accompanied by emission of a quantum. This luminescence centre is probably observed in our polycrystalline CVD ZnSe. It causes a wide band with the maximum located at 630 nm (1.98 eV). The authors of Ref. [22–24] believe that the corresponding emission region can vary from 615 to 650 nm for different samples.

We have also studied the dependence of radiation intensity on the excitation power (Nd:YAG laser at λ_{ex} = 532 nm). The appropriate results are depicted in Fig. 11. They concern a fixed wavelength corresponding to the maximum located at 650 nm (see Fig. 8). The radiation intensity at the maximum (λ_{max} = 650 nm) increases almost linearly over a wide region of changes in the excitation power (from 1 to 10 mW). Then it becomes saturated due to decreasing recombination output through so-called r-recombination centres. This is because of a high level of luminescence excitation, when the r-centres are strongly filled with holes. It can be assumed that the linear increase in the intensity occurring with increasing pumping is due to the fact that directly excited carriers participate in the process of recombination radiation. Then the number of centres, which are populated under equilibrium conditions and are responsible for the luminescence, does not change.

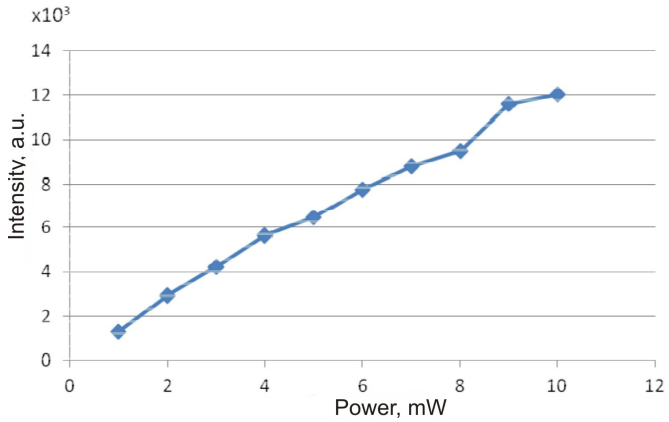

Fig. 11. Dependence of radiation intensity corresponding to λ_{max} = 650 nm (see Fig. 8) on the power of excitation source (laser at λ_{ex} = 532 nm).

To describe the typical recombination luminescence processes occurring in polycrystalline CVD-ZnSe, we have used a particular band-theory model suggested in Ref. [24]. Following from the experimental luminescence spectra that correspond to excitations through the polished and unpolished surfaces of our sample, we can claim the following statements:

(1) When observing the PL in polycrystalline CVD ZnSe at the wavelengths 430, 433 and 443 nm ('purple' peaks), 451 nm ('blue' band) and 458 nm ('blue' line), we deal with the 'edge' luminescence associated with Zn vacancies [4]. The first three peaks arise from the excitation of our sample with the laser (λ_{ex} = 325 nm) and the last two arise from the excitation with the xenon lamp (λ_{ex} = 325 and 330 nm). The 'edge' luminescence also prevails in the wavelength region 460÷486 nm. It is caused by the excitons bound to various impurities and defects [9, 10, 12, 19, 20]. In the case of polished sample surface, the lines located at 478 and 483 nm ('blue' and 'light blue' bands) and at 486 nm ('blue' peak) correspond to the excitons bound to different impurities. In the case of unpolished surface, one observes a single line, a peak located at 443 nm.

If compared with the case of polished surface, the intensity of certain lines in the latter case decreases or the lines disappear at all. This is due to their strong absorption in the crystal.

(2) The 'green' band observed in the region 500÷590 nm is, most likely, related to the luminescence of impurity-defect complexes [9, 10, 12, 16]. The 'green' band observed from the unpolished surface of our sample is shifted towards longer wavelengths with respect to the 'green' band observed from the polished surface. It is known that the complexes of intrinsic point defects with oxygen and the other background impurities can have slightly different modifications, which is related to the fact that the distances between the elements of the complexes are different, and there can be different concentrations of complexes in different geometries of the sample under study. This results in varying energy levels. As a consequence, one can explain in this manner large widths of the luminescence bands and changes in their shapes under conditions when different points at the sample surface are studied. It is also conceivable that the formation of a damaged layer during mechanical polishing must lead to a sharp decrease in the lifetime of charge carriers and a decrease in both the 'edge' luminescence and the other luminescence types.

(3) The 'red' luminescence band is observed in the region 625÷730 nm. It is still *due to* the impurity-defect complexes. However, it differs in its structure and character from the luminescence linked with the complexes that determine the 'green' band [9–11, 16, 23–25]. In the luminescence spectra observed upon the laser excitation at λ_{ex} = 325 nm in the two alternative cases, the 'red' band is almost the same – there is no particular difference. On the contrary, when the sample is excited by the semiconductor laser (λ_{ex} = 532 nm) in the both cases and with the laser of the same wavelength from the unpolished sample surface, the 'red' band in the luminescence spectrum is significantly different, i.e. the spectral position of its maximum and the half-width of the band change notably. It is evident that the wide emission bands typical for polycrystalline CVD ZnSe in the wavelength region 615÷650 nm are not elementary. They are associated with the recombination luminescence centres. Then the two opposite recombination mechanisms can occur simultaneously, which are linked with either electron or hole. In the present work, we have also studied the dependence of the radiation intensity at a fixed wavelength, which corresponds to the spectral maximum 650 nm, on the excitation power. This is a kind of lux–ampere characteristic at the radiation wavelength 650 nm, which is almost linear.

(4) The 'infrared' luminescence bands with the maxima centred at 824, 970, 1230 and 1423 nm are observed from the polished sample surface upon the excitation by the semiconductor lasers with the wavelengths λ_{ex} = 532, 642 and 785 nm. In the case of unpolished sample surface, only a single peak at 810 nm is observed, when the sample is excited by the laser with the wavelength λ_{ex} = 532 nm. All of these luminescence bands are related to selenium vacancies V_{Se}. It is worthwhile in this respect that the authors of Refs. [17, 21] have earlier demonstrated that the band intensity increases with increasing Se excess, i.e. with increasing concentration of zinc vacancies [V_{Zn}].

4. Conclusions

As a result of our experimental data and its analysis, the following conclusions can be made.

1. The 'edge' luminescence dominates in the wavelength regions 430÷451 nm and 460÷486 nm. Here different lines observed in the case of polished sample surface are due to the excitons bound at different impurities and defects. In the case of unpolished sample surface, only one line is observed, the peak located at 443 nm. The decrease in the intensity of certain lines or their disappearance in the latter case is due to their strong absorption in the crystal.

2. The ‘green’ band in the region 500÷550 nm detected in case of the unpolished surface of our sample is shifted towards longer wavelengths with respect to the ‘green’ band observed from the polished surface. It can be assumed in this respect that the complexes of intrinsic point defects with oxygen and the other background impurities can have slightly different modifications. This is associated with the fact that the distances between the elements of these complexes are different and, moreover, there can be different concentrations of these complexes in different geometries. This yields in varying energy levels. On this basis one can explain a large width of the luminescence band and the change in its shape which occur when different points at the sample surface are tested.

3. The ‘red’ band in the luminescence spectra observed upon the laser excitation at λ_{ex} = 325 nm ($h\nu_{ex} > E_g$) remains almost the same in the both alternative cases. When the sample is excited by the semiconductor laser at λ_{ex} = 532 nm ($h\nu_{ex} < E_g$) in these cases or by the laser of the same wavelength from the unpolished surface, the ‘red’ bands in the luminescence spectra are significantly different. Namely, the spectral positions of the maxima and the half-widths of these bands change notably. One can also note that the wide emission bands detected for polycrystalline CVD ZnSe in the wavelength region 615÷650 nm are not elementary.

4. The ‘infrared’ luminescence bands with the maxima located at the wavelengths 970, 1225 and 1420 nm are observed from the polished surface of our sample upon the excitation by the semiconductor lasers with the wavelengths λ_{ex} = 532, 642 and 785 nm ($h\nu_{ex} < E_g$). On the other hand, a single peak at the wavelength 810 nm is observed in case of the unpolished surface, when the sample is excited by the laser at λ_{ex} = 532 nm. Different maxima observed in this case are due to the fact that the deviations from stoichiometry in different geometries of the test sample are not the same.

Acknowledgement

The authors express their gratitude to Prof. N. Mehdiyev for interesting discussions.

References

1. Georgobiani A N, Kotlyarevsky M B, 1985. Problems of creation of injection LEDs based on wide bandgap semiconductor compounds. Izv. AN USSR. Ser. Phizika. **49**: 1916-1922.
2. Il'chuk G A , Rud' V Yu , Rud' Yu V, Bekimbetov R N , Ivanov-Omskiy V I , Ukrainets N A, 2000. Photosensitivity of structures based on ZnSe single crystals. Semiconductors. **34**: 781-785.
3. Berezhnoi K V, Nasibov A S, Shapkin P V, ShpakV G, Shunqylov S A,Yalandin M I, 2008. Emission of zinc selenide plates excited by a pulsed electric field. Quantum Electronics. **38**: 829-832.
4. Edgar Mosquera, Nicolás Carvajalb, Mauricio Morelb and Carlos Marín, 2017. Fabrication of ZnSe nanoparticles: Structural, optical and Raman Studies, Journal of Luminescence. **192**: 814-817.
5. Billie L Abrams and Paul H Holloway, 2004. Role of the surface in luminescent processes. Chem. Rev. **104**: 5783-5802.
6. Manhas M, Vinay Kumar, Ntwaeaborwa O M, and Swart H C, 2016. Structural, surface and luminescence properties of $Ca_3B_2O_6:Dy^{3+}$ phosphors**.** Ceramics International. **42**: 5743-5753.
7. Devyatykh G G, Gavrishchuk Ye M and Dadanov A Yu, 1990. Study of the kinetics of zinc selenide chemical deposition from the gas phase in a horizontal flow reactor. High-Purity Substances. **2**: 174-179.

8. Hartman H, Hildisch L, Krause E and Mohling W, 1991. Morphological stability and crystal structure of CVD grown zinc selenide. J. Mater. Sci. **26**: 4917-4923.
9. Nedeoglo D D and Simashkevich A V. Electric and luminescent properties of zinc selenide. Kishinyov: Shtiintsa (1984).
10. Gavrilenko V I, Grekhov A M, Korbutyak D V, Litovchenko V G. Optical properties of semiconductors: handbook. Kiyev: Naukova dumka (1987).
11. Vaksman Yu F, Nitsuk Yu A, Yatsun V V, Nasibov A S, Shapkin P V, 2011. Effect of iron impurities on the photoluminescence and photoconductivity of ZnSe crystals in the visible spectral region. Semiconductors. **45**: 1129-1132.
12. Gladilin A A , Il'ichev N N, Kalinushkin V P, Studenikin M I, Uvarov O V, Chapnin V A, Tumorin V V i Novikov G G. 2019. Study of the Effect of Doping with Iron on the Luminescence of Zinc-Selenide Single Crystals. Semiconductors. **53**: 1-8.
13. Qi Zhang, Huiqiao Li, Ying Ma and Tianyou Zhai, 2016. ZnSe nanostructures: synthesis, properties and applications. Prog. Mat. Science. **83**: 472–535.
14. Makhniy V P, Kinzerskaya O V, Senko I M and Slotov A M, 2016. High temperature luminescence of ZnSe:Yb crystals. Technology and design in electronic equipment. **2-3**: 37-40.
15. Chan K K, Mozhevitina Ye N, Khomyakov A V, Kobeleva S P and Avetisov I Kh, 2013. Nonstoichiometry and luminescence of crystalline ZnSe. Advances in chemistry and chemical technology. **27**: 64-69.
16. Morozova N K, Mideros D A , Gavrishchuk E M, Galstyan V G, 2008. Role of background O and Cu impurities in the optics of ZnSe crystals in the context of the band anticrossing model. Semiconductors. **42**: 131-136.
17. Morozova N K, Karetnikov I A, Blinov V V, Gavrishchuk E M, 2001. Studies of the infrared luminescence of ZnSe doped with copper and oxygen. Semiconductors. **35**: 512 -515.
18. Vil'chinskaya S S, Oleshko V I , Gorina S G, 2011. Low-temperature luminescence of zinc selenide crystals grown by various methods. Izv. vuzov. Ser. Physics. **54**: 138-142.
19. Grivul V I, Makhniy V P, Slyotov M M, 2007. The origin of edge luminescence in diffusion ZnSe:Sn layers. Semiconductors. **41**: 784-785.
20. Saxena A, Yang S, Philipose U and Ruda H E, 2008. Excitonic and pair-related photoluminescence in ZnSe nanowires. J. Appl. Phys. **103**: 053109 (1–7).
21. Degoda V Y, Sofiyenko A O, 2010. Specific features of the luminescence and conductivity of zinc selenide on exposure to X-ray and optical excitation. Semiconductors. **44**: 568-574.
22. Degoda V Ya, Pavlova N Yu, Podust G P , Sofiienko A O, 2015. Spectral structure of the X-ray stimulated phosphorescence of monocrystalline ZnSe. Physica B: Condensed Matter. **465**: 1-6.
23. Alizadeh M, Degoda V Ya, Kozhushko B V, Pavlov N Yu, 2017. Luminescence of dipole-centers in ZnSe crystals. Functional Materials. **24**: 206-211.
24. Triboulet R and Siffert P. CdTe and related compounds; physics, defects, hetero- and nanostructures, crystal growth surfaces and applications. Oxford: Elsevier (2010).

Abbasov I., Musayev M., Huseynov J., Kostyrko M., Babayev S., Eyyubov G. and Aliyeva S. 2020. Photoluminescence spectra of polycrystalline ZnSe in different experimental geometries. Ukr.J.Phys.Opt. **21**: 103 – 114 doi: 10.3116/16091833/21/2/103/2020

Анотація. *Вивчено фотолюмінесценцію полікристалічного ZnSe, синтезованого за допомогою методу хімічного висадження з парової фази, яка виникає внаслідок збудження джерелами різних типів з різними довжинами хвиль. Використано дві експериментальні*

геометрії, пов'язані з нормальним падінням випромінювання збудження на поліровану або неполіровану поверхні ZnSe. Збудження з боку полірованої поверхні здійснювали лазерами з довжинами хвиль λ_{ex} = 335 і 325 нм (з енергіями фотона, які перевищують ширину забороненої зони, тобто $h\nu_{ex} > E_g$), напівпровідниковими лазерами з λ_{ex} = 532, 642 і 785 нм (тобто, $h\nu_{ex} < E_g$) і ксеноновою лампою. Зразок також збуджували з боку неполірованої поверхні, використовуючи лазери з λ_{ex} = 325 нм ($h\nu_{ex} > E_g$) і λ_{ex} = 532 нм ($h\nu_{ex} < E_g$), а також напівпровідниковий лазер з λ_{ex} = 532 нм ($h\nu_{ex} < E_g$). На основі результатів експериментів проаналізовано та порівняно крайову (екситонну) люмінесценцію та люмінесценцію, пов'язану з домішковими дефектами. Виявлено різні типи поведінки спектрів люмінесценції, які залежать від типів збудження.